DUST

Minor component of ISM by mass: ~1:100 of gas mass in MW
Major reservoir of refractory elements: depleted from gas phase
Major donor of electrons: dominates the thermal balance, couples radiation field to gas.

Extinction:

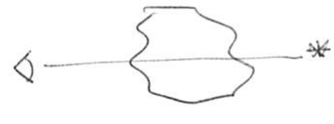

$$F_{with} = e^{-\tau} \cdot F_{w_o}$$

$$\Delta m = -2.5 \log_{10}\left(\frac{F_{with}}{F_{w_o}}\right) = -2.5 \log e^{-\tau} = \tau \cdot 2.5 \log e$$
$$= 1.086\,\tau$$

$\Rightarrow A_\lambda = 1.086\,\tau_\lambda$ "general extinction"

Difficult to measure: it is easier to measure the "selective extinction" or "reddening": $E(\lambda_1, \lambda_2) = A_{\lambda_1} - A_{\lambda_2}$

$\Rightarrow$ difference between extincted an unextincted object

E.g.: $E_{B-V} = A_B - A_V$ $\quad \lambda_B = 4350$ Å
$\lambda_V = 5550$ Å

$$= 1.086\,(\tau_B - \tau_V)$$

Measurements find $\langle E_{B-V} \rangle = 0.61 \frac{mag}{kpc} \cdot L$ in Gal. plane

If gas and dust have the same D/G in atomic and molecular material,

$$N_H = (N_{HI} + 2N_{H_2}) = 5.8 \times 10^{21}\, E_{B-V}\ mag^{-1}\, cm^{-2}$$

Bohlin, Savage, & Drake (1978)

deviations exist, grain growth?

We'll see next that extinction → 0 for $\lambda \to \infty$ since $\lambda \gg$ grain size (e.g., $\sigma_{sca} = \left(\frac{a}{\lambda}\right)^4$ for Rayleigh scat)

$$\Rightarrow E_{\infty,V} = A_{\lambda\to\infty} - A_V = -A_V$$

Define $R_V \equiv -\frac{E_{\infty,V}}{E_{B-V}} = \frac{A_V}{E_{B-V}}$

⇒ Observations of $E_{\lambda,V}$ at large wavelength can be used to determine R_V. Typical $R_V \approx 3.1$ with some dispersion along different l.o.s.

⇒ $A_V = R_V E_{B-V}$ ⇒ $N_H = 1.9 \times 10^{21} A_V \text{ mag}^{-1} \text{ cm}^{-2}$ (Bohlin 1978)

Typical HI clouds have $N_H = 10^{20}$ ⇒ $A_V = 0.1$ (Transparent). Molec. clouds have $N_H = 10^{22}$ ⇒ $A_V = 10$, light intensity is reduced by $\sim e^{-10} \sim 10^{-5}$!

Combining $E_{B-V}(R)$ and $N_H(E_{B-V})$ ⇒ $\langle n_H \rangle = 1.2 \text{ cm}^{-3}$

$$\sigma_{grain} = \sigma_{geom} \cdot Q_e$$

"effective area"; $\sigma_{geom} = \pi a^2$; Q_e = efficiency factor

$$Q_e = Q_s + Q_a$$

(Q_s: scattering, Q_a: absorption)

For $a \ll \frac{\lambda}{2\pi}$ (grains are $\lesssim 0.1\,\mu m = 10^{-5}$ cm, $\frac{\lambda}{2\pi} > 10^{-5}$ for optical wv.)

Mie Theory gives:

$$Q_s = \frac{8}{3}\left(\frac{2\pi a}{\lambda}\right)^4 \left|\frac{\varepsilon - 1}{\varepsilon + 1}\right|^2$$

→ Rayleigh scattering

$$Q_a = \frac{2\pi a}{\lambda} \cdot 4 \cdot \text{Im}\left(\frac{\varepsilon - 1}{\varepsilon + 2}\right)$$

ε = complex dielectric constant $\cong$ square of index of refraction

$n = \sqrt{\varepsilon \mu}$ $\mu \approx 1$

⇒ @ $\frac{2\pi a}{\lambda} \ll 1$, $Q_a \gg Q_s$ ⇒ most extinction is due to absorption

$Q_a \propto a$ (radius) ⇒

$\sigma_{grain} \propto a^2 \cdot a \propto a^3 \propto$ mass

"effective area xsection"

⇒ Extinction $\propto$ to mass along los when $\lambda \gg a$ (IR)

$A_\lambda = 1.086 \cdot n_{gr} \cdot L \cdot \sigma_g \propto N_{grain} \cdot \text{mass} \propto$ mass/area in grains

(n_{gr}: volume # density; σ_g: ∝ mass of a grain; N_{grain}: #/area)

⇒ $A_\lambda / m_H \cdot N_H$ @ λ big gives dust-to-gas ratio, ≈ 0.01

Since $Q_s \propto \left(\frac{a}{\lambda}\right)^4$, scattering dominated by large grains

$\sigma_{grain,\,scat} \propto a^6$

Since $\sigma_{grain} \uparrow$ with $\lambda \downarrow$, $A_\lambda \uparrow$ for $\lambda \downarrow$

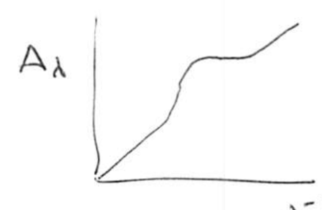

Features: (a) UV peak @ 2175 Å
(small carbonaceous grains) Li & Draine 2000

(b) IR features @ 9.7 and 18 μm
(amorphous silicates like olivine)

(c) "PAH" or "aromatic" features 7.7, 11.3, 17 μm, etc

(d) Many DIBS

(a) → $a < 15$ nm, $\lesssim 500$ C atoms, requires %15 of C to be in this form of "aromatic" rings

Emission: UV, optical absorbed ⇒ re-emitted in the IR

$$E_{abs}/s/cm^2 = \pi \int J_\nu d\nu$$

$$E_{em}/s/cm^2 = \pi \int B_\nu(T_d) d\nu$$

$$\Rightarrow \pi \int B_\nu(T_d) d\nu = \sigma_{SB} T_d^4 \Rightarrow T_d = \left(\frac{\pi \int J_\nu d\nu}{\sigma_{SB}} \right)^{1/4}$$

~~"classical" grains in equilibrium with Radiation~~

$$U_\nu = \frac{\int I_\nu d\Omega}{c} \quad \text{energy density of rad.} = \frac{4\pi}{c} J_\nu$$

$$U = \frac{G_0 \cdot 4\pi}{c}$$

$$\Rightarrow T_d = \left(\frac{c}{4\pi} \frac{\pi}{\sigma_{SB}} \int U_\nu d\nu \right)^{1/4}$$

"$\frac{erg}{cm^3}$" $\approx 7 \times 10^{-13}$ for Habing field

For $G_0 \sim 1.7 \times 1.6 \times 10^{-3}$ erg cm^{-2} s^{-1} (mean ISRF)

$T_d \sim 3\text{-}3.5$ K ⟩ Clearly wrong for Black Body. why?

In fact, only a fraction of starlight is absorbed

Kirchoff's law, $\frac{j_\nu}{4\pi} = K_\nu B_\nu(T)$ for dust @ Temperature T

$$\Rightarrow \int_0^\infty C_{abs}(a,\lambda)\, c \cdot U_\lambda \, d\lambda = \int_0^\infty C_{abs}(a,\lambda) \cdot 4\pi B_\lambda(T)\, d\lambda$$

Typical equil. Temp. is $T_d \sim 10\text{-}25$ K for sizes 0.01-1μm with graphite slightly hotter than silicates and average interstellar rad field. ⇒ pervasive FIR emission

These are "classical" big grains in equilibrium w/rad. field

Small grains, however, never reach equilibrium

T spikes when photon is absorbed

$E_\gamma = 10\,eV$

$\Rightarrow T = \frac{10\,eV}{3N\,k} \simeq \frac{40{,}000}{N}\,K \Rightarrow$ if $N \sim 100 \Rightarrow T \uparrow$ several hundreds

↑ DOF

when photon absorbed

"aromatic"

Observed IR features arise from this process.

These are "stochastically heated" grains

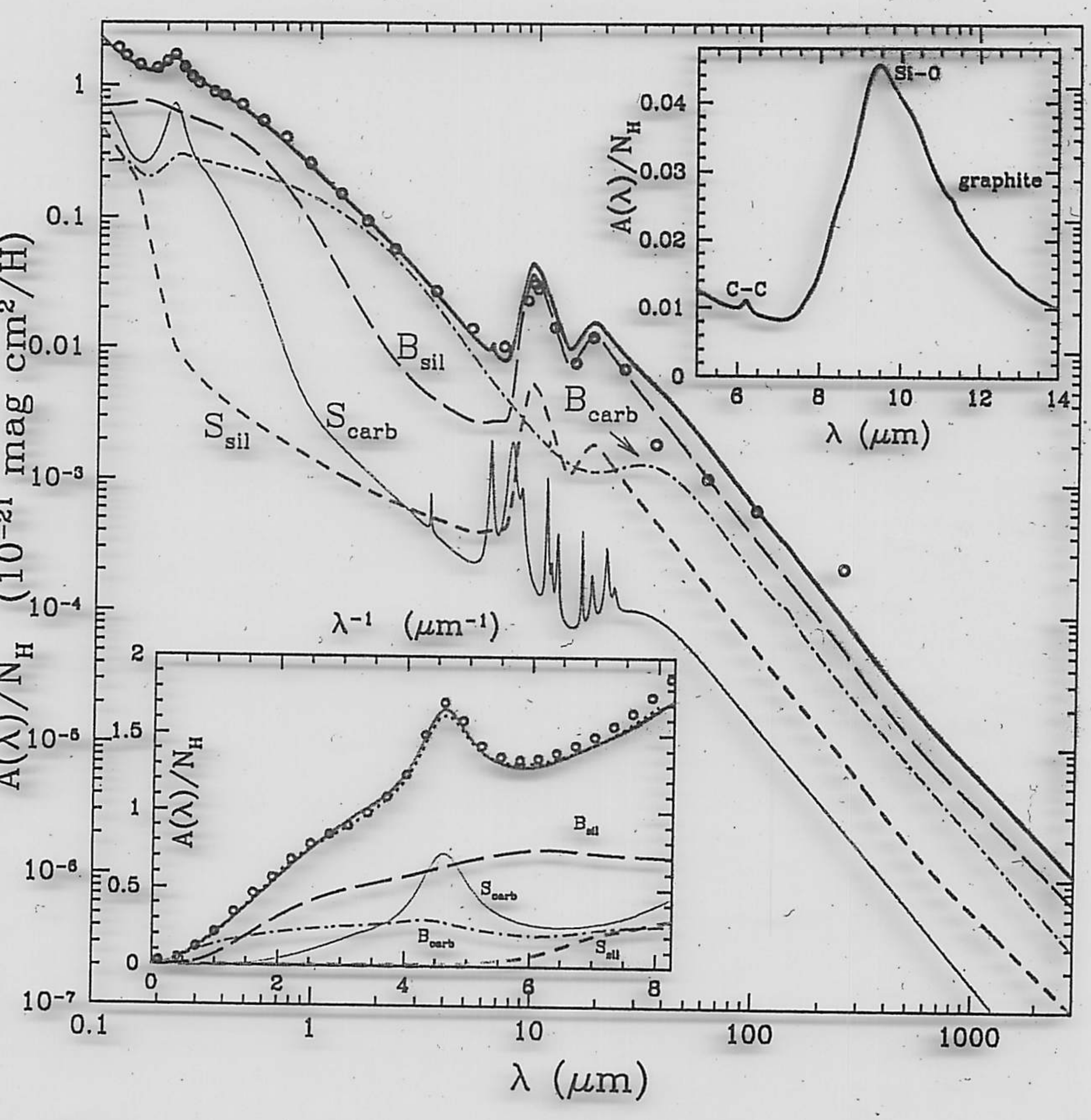

Fig. 16.— The calculated extinction for the present grain model (heavy solid line) and the observed average ($R_V \approx 3.1$) interstellar extinction curve (dotted line: Fitzpatrick 1999; open circles: Mathis 1990). Model results are the sum of 4 components: "B_{sil}" (silicate, $a \geq 250$Å; long-dashed line); "S_{sil}" (silicate, $3.5 \leq a \leq 250$Å; short-dashed line); "B_{carb}" (carbonaceous, $a \geq 250$Å; dot-dashed line); and "S_{carb}" (carbonaceous, $3.5 \leq a \leq 250$Å, including PAHs; thin solid line). The upper-right inset illustrates the aromatic 6.2μm absorption feature and the 9.7μm silicate band. The narrow feature at 11.5μm is due to a lattice mode of crystalline graphite (Draine 1984) and would likely be smoothed out in an imperfect polycrystalline sample. The lower-left inset plots the extinction curve against λ^{-1} (μm^{-1}).

Extinction Curve - Diffuse ISM

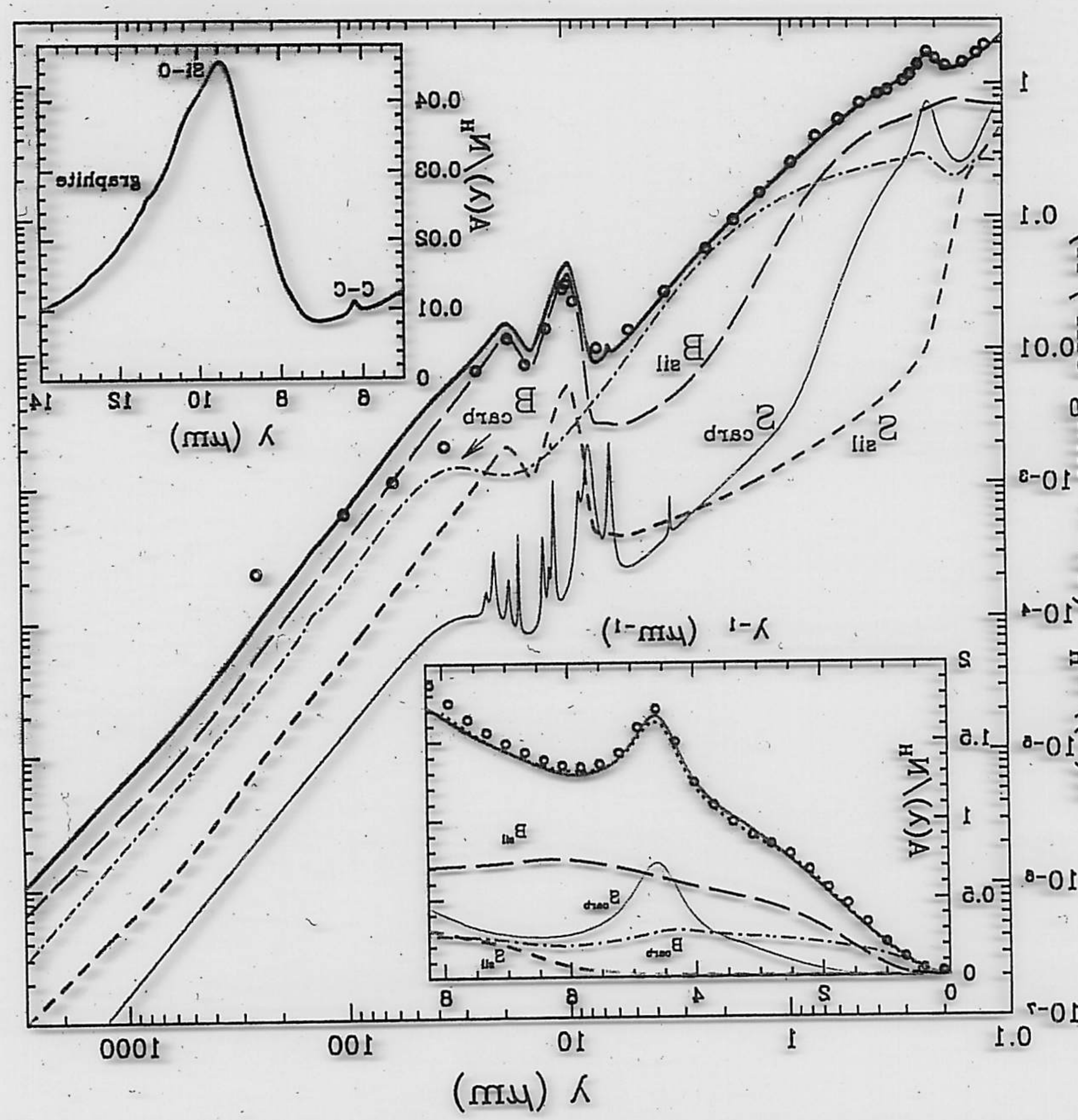

Fig. 16.— The calculated extinction for the present grain model (heavy solid line) and the observed average ($R_V \approx 3.1$) interstellar extinction curve (dotted line: Fitzpatrick 1999; open circles: Mathis 1990). Model results are the sum of 4 components: "B_{sil}" (silicate, $a \geq 250$Å; long-dashed line); "S_{sil}" (silicate, $3.5 \leq a \leq 250$Å; short-dashed line); "B_{carb}" (carbonaceous, $a \geq 250$Å; dot-dashed line); and "S_{carb}" (carbonaceous, $3.5 \leq a \leq 250$Å, including PAHs; thin solid line). The upper-right inset illustrates the aromatic 6.2μm absorption feature and the 9.7μm silicate band. The narrow feature at 11.5μm is due to a lattice mode of crystalline graphite (Draine 1984) and would likely be smoothed out in an imperfect polycrystalline sample. The lower-left inset plots the extinction curve against λ^{-1} (μm^{-1}).

Extinction Curve - Diffuse ISM

MRN = Mathis, Rumpl, Nordsieck 1977

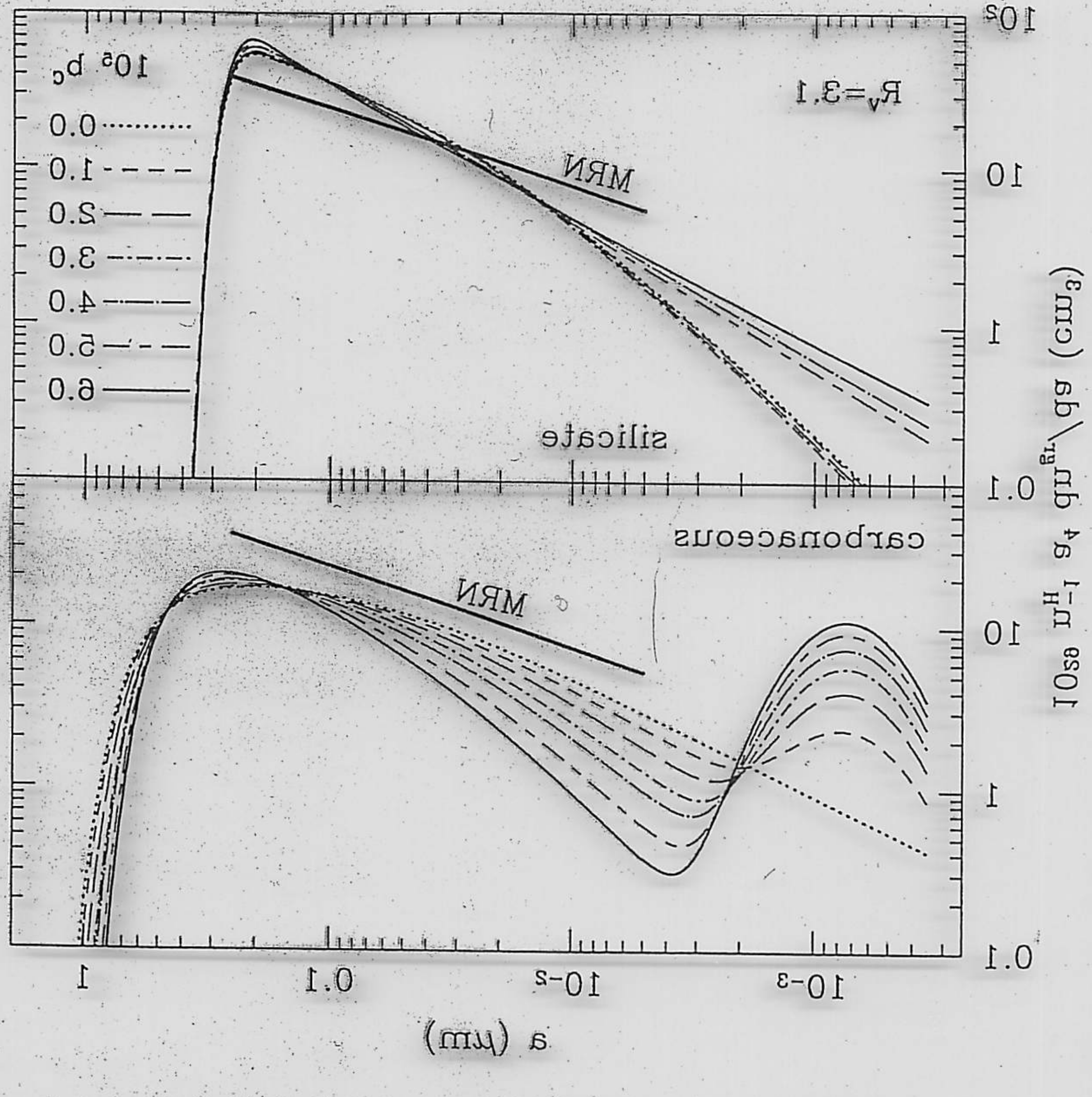

Fig. 2.— Case A grain size distributions for $R_V = 3.1$. The values of b_C are indicated. The heavy, solid lines are the MRN distribution, for comparison. Our favored distribution has $b_C = 6 \times 10^{-5}$ (see text).

MRN = Mathis, Rumpl, Nordsieck 1977

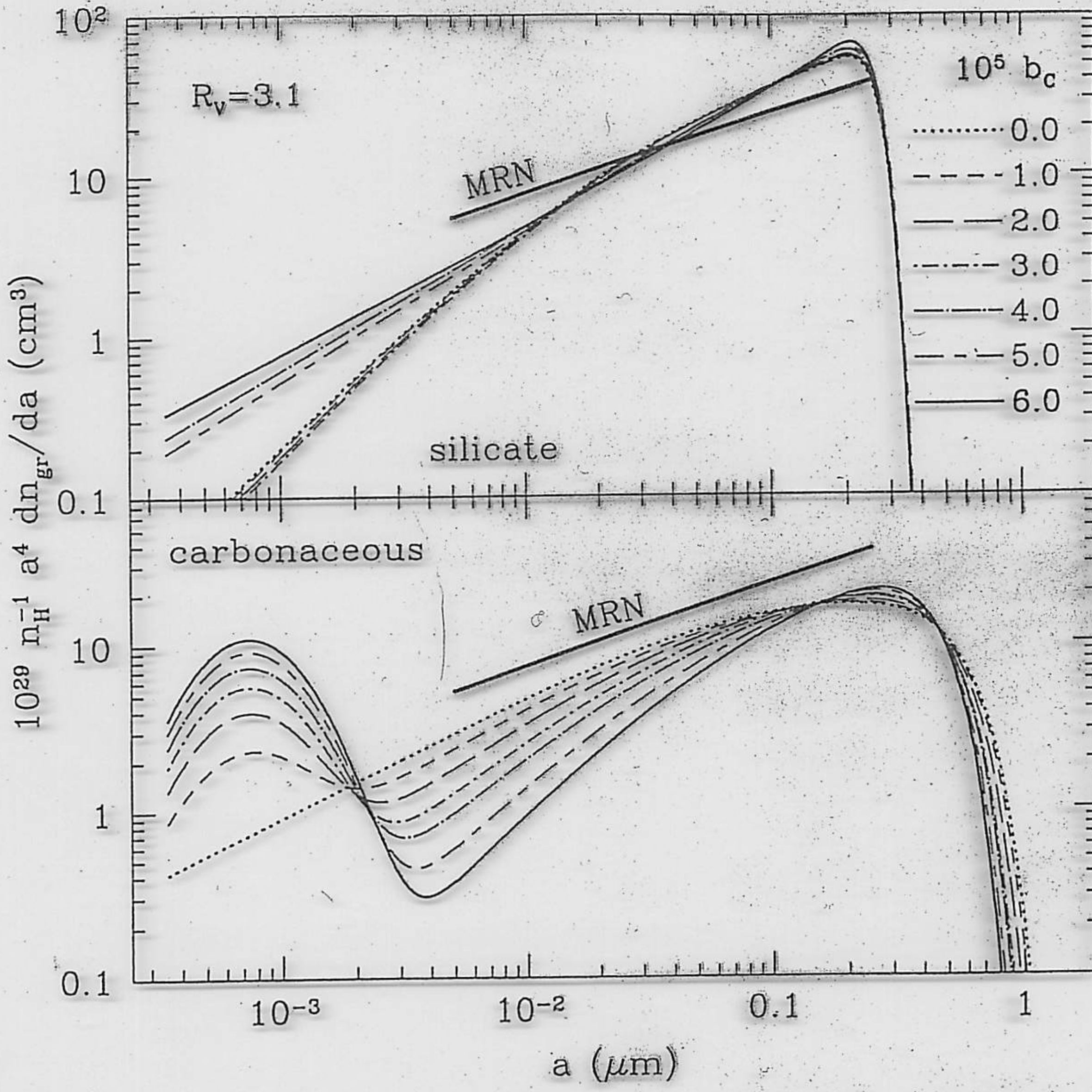

Fig. 2.— Case A grain size distributions for $R_V = 3.1$. The values of b_C are indicated. The heavy, solid lines are the MRN distribution, for comparison. Our favored distribution has $b_C = 6 \times 10^{-5}$ (see text).

AVERY® PV11$

Draine & Lee 1984
Li & Draine 2000

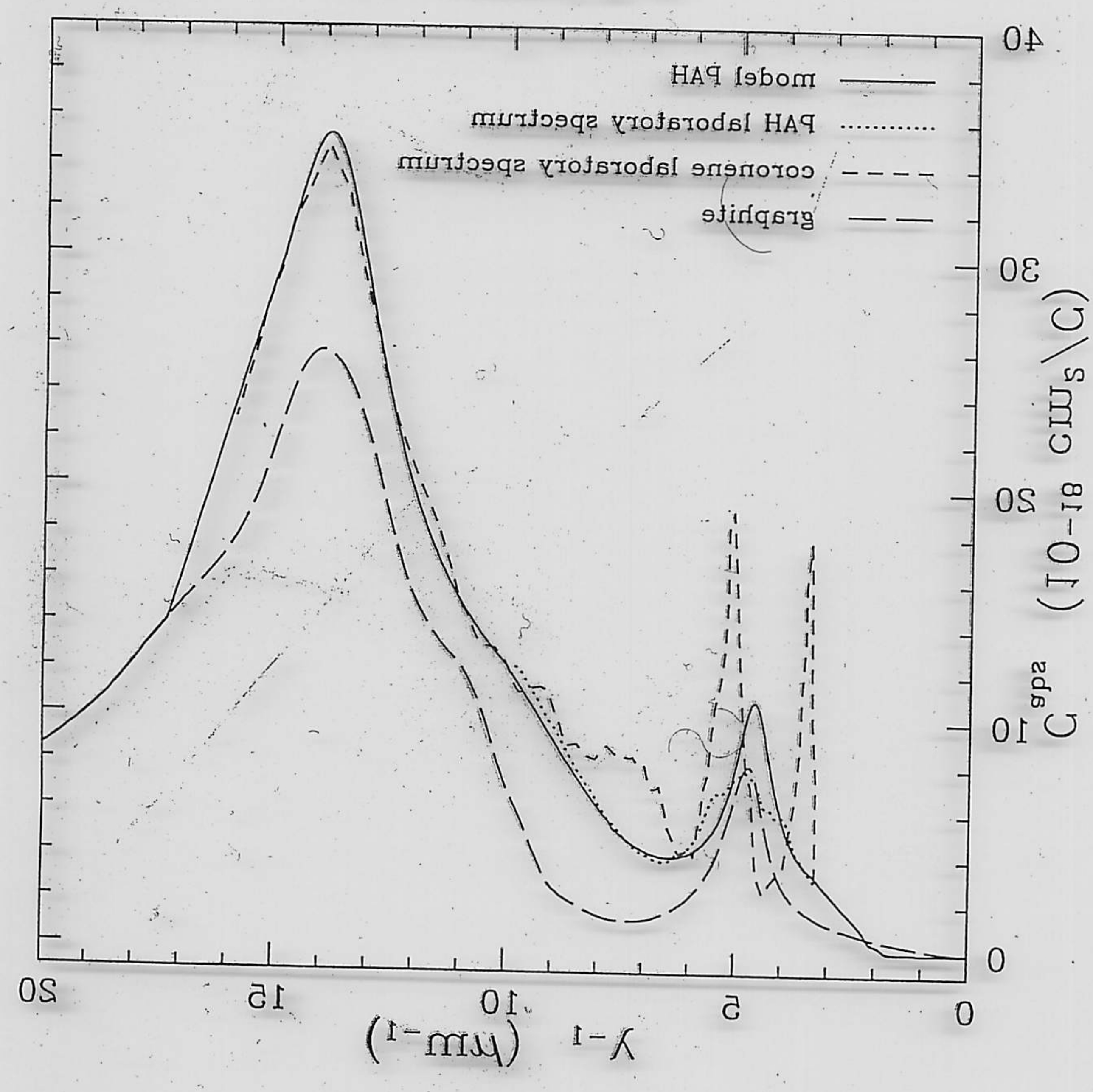

Fig. 1.— The ultraviolet and far ultraviolet absorption spectrum of PAHs.

Draine & Lee 1984
Li & Draine 2000

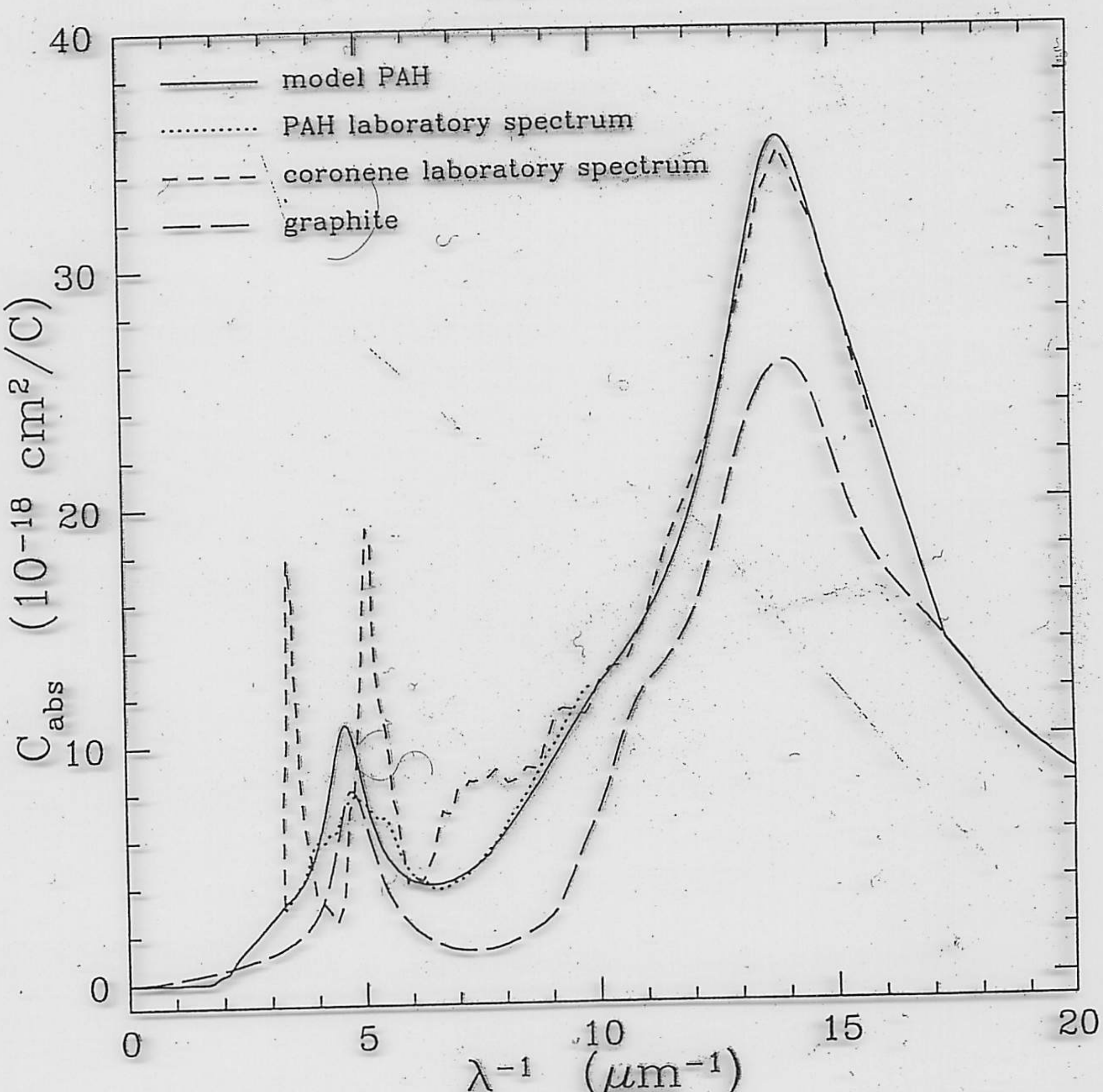

Fig. 1.— The ultraviolet and far ultraviolet absorption spectrum of PAHs.

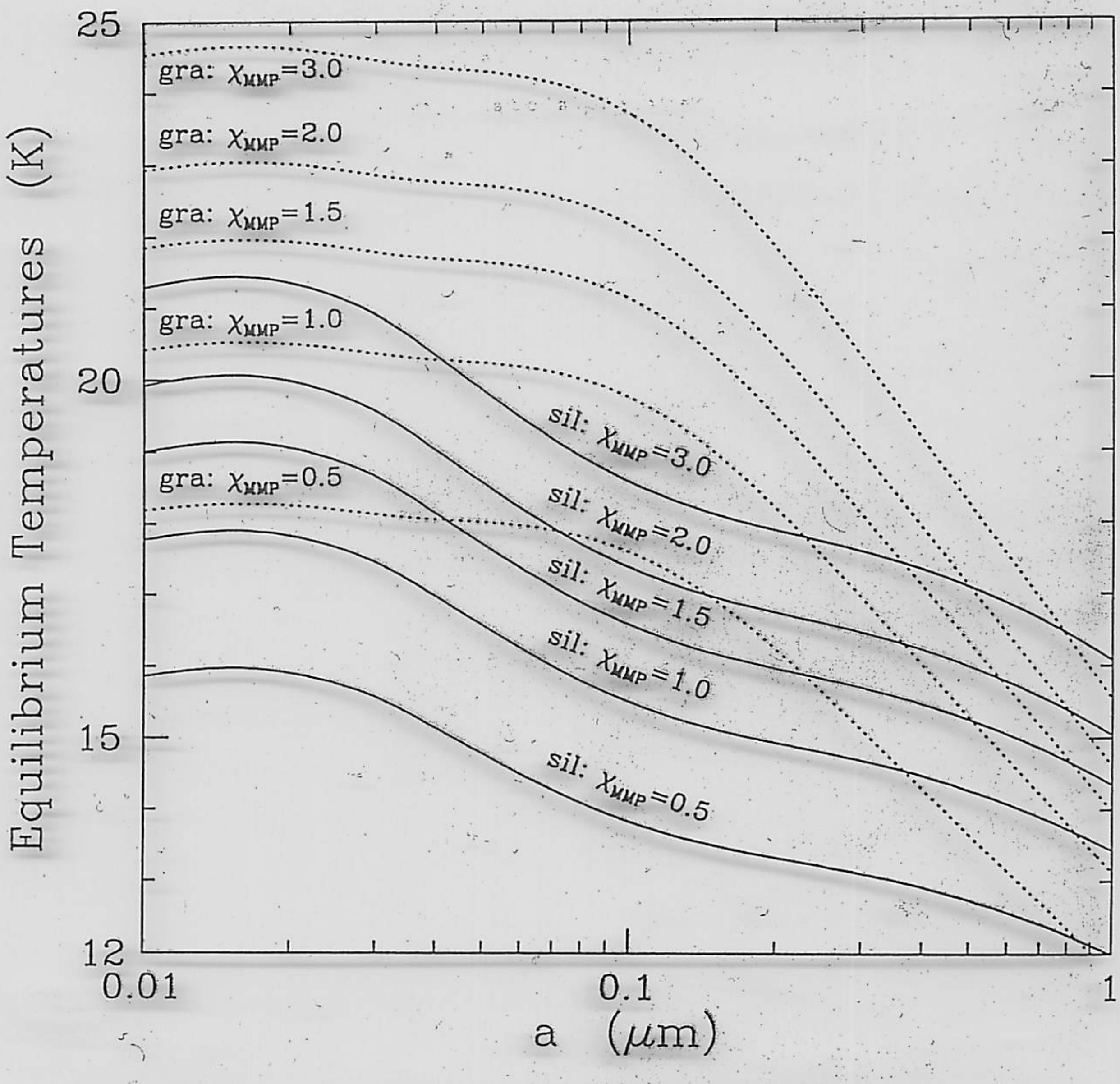

Fig. 3.— Equilibrium temperatures for graphite (dotted lines) and silicate grains (solid lines) in environments with various starlight intensities.

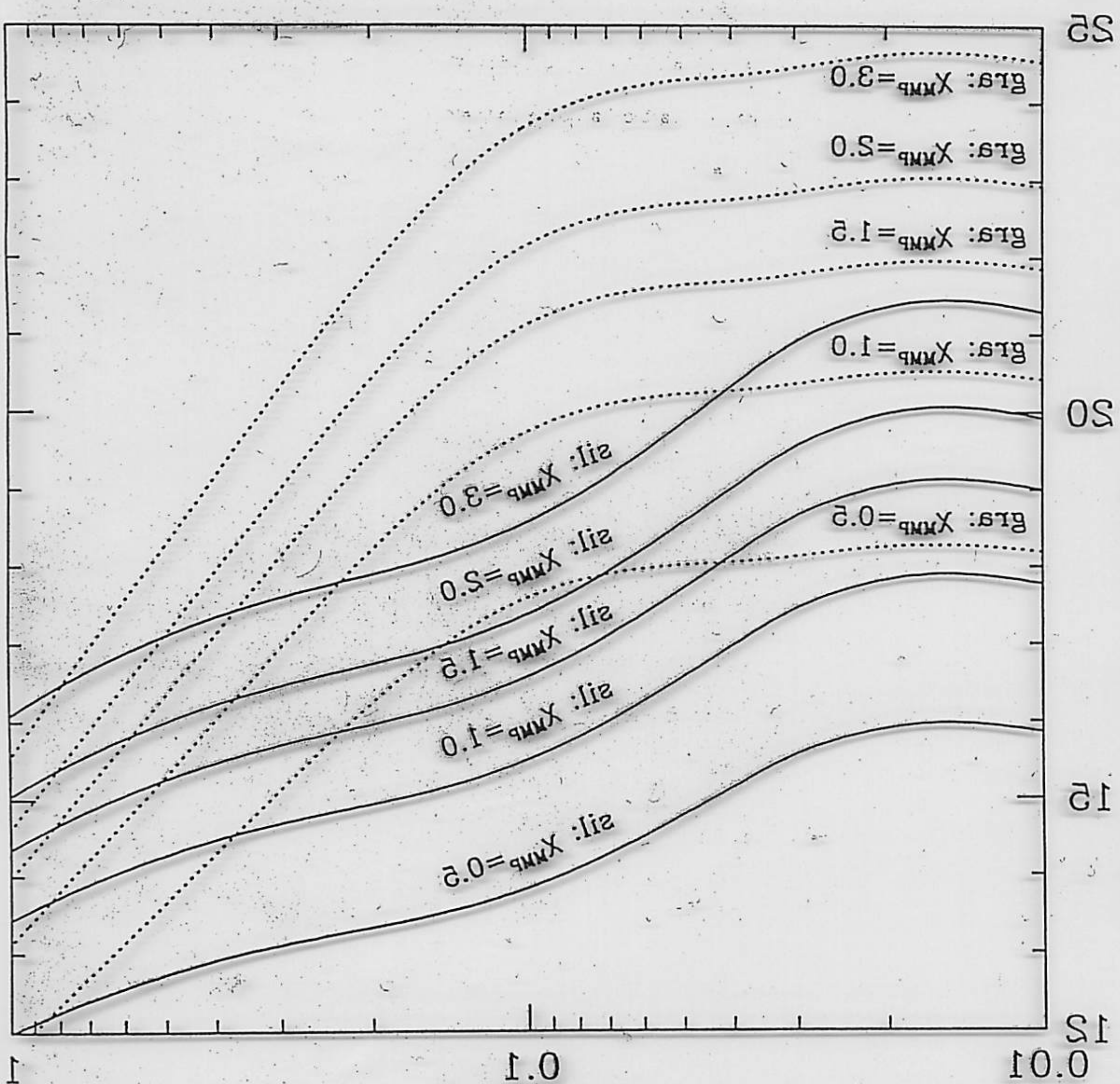

Fig. 3.— Equilibrium temperatures for graphite (dotted lines) and silicate grains (solid lines) in environments with various starlight intensities.

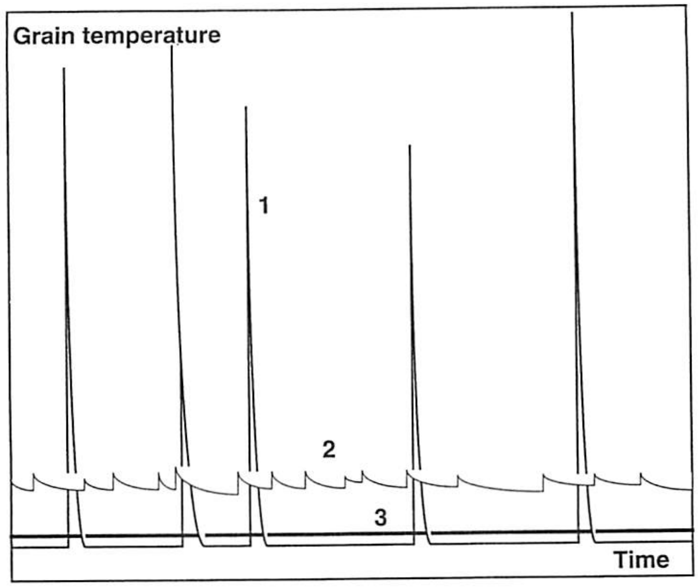

Fig. 7.10. Scheme for the time evolution of the temperature, hence of the emitted intensity for grains of different sizes, submitted to the interstellar radiation field. The big grains (broad horizontal line, 3), are in thermal equilibrium and their temperature, hence the emitted intensity, does not vary. The smallest grains experience an immediate, very strong increase in temperature after absorption of a photon, and rapidly cool down to a low temperature (1). The temperature of intermediate-size grains increases slightly after each photon absorption, causing temperature fluctuations less pronounced than in the preceding case (thin line, 2). The scales are arbitrary and different for each case.

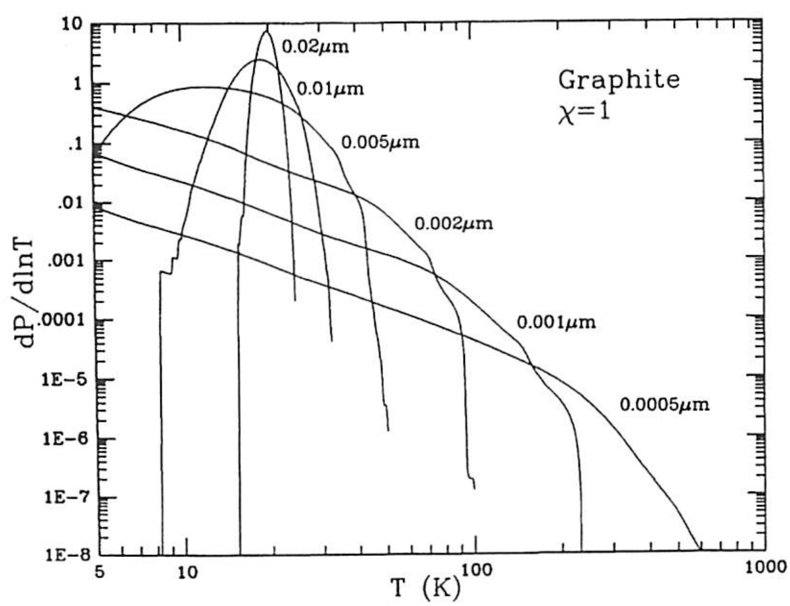

Fig. 7.11. Temperature distributions $dP/d\ln T$ for graphite grains of various radii a exposed to the interstellar radiation field near the Sun. $P(T)$ is the probability that a grain will have a temperature larger than T. Note that the big grains are approximately in equilibrium at a temperature of about 20 K. Reproduced from Draine & Anderson [135], with the permission of the AAS.